DEPARTMENT OF DEFENCE
DEFENCE SCIENCE & TECHNOLOGY ORGANISATION
DSTO

Modelling Acoustic Backscatter from Near-Normal Incidence Echosounders - Sensitivity Analysis of the Jackson Model

P. J. Mulhearn

DSTO-TN-0304

Modelling Acoustic Backscatter from Near-Normal Incidence Echosounders - Sensitivity Analysis of the Jackson Model

P. J. Mulhearn

Maritime Operations Division
Aeronautical and Maritime Research Laboratory

DSTO-TN-0304

ABSTRACT

For a number of years systems, such as RoxAnn and QTC-View, have been attached to ships' echosounders in order to estimate sediment bottom types from the acoustic returns. In this report the physics of acoustic backscatter is examined, at near-normal incidence grazing angles, to determine if these systems can be made less empirical. The Jackson model is used to examine backscatter versus grazing angle, for angles between 65 and 90 degrees, at a frequency of 50 kHz. This is a typical frequency for a standard ship's echosounder. Backscatter predicted by the Jackson model depends on six input parameters and a range of different physical mechanisms. In order to simplify interpretation of results, it seems worthwhile to examine the sensitivity of the model results to different input parameters as a function of sediment type. It is likely that not all six parameters will always be needed, and that some scattering mechanisms can be ignored in some cases. Backscatter versus time for a pulsed system will be examined in a subsequent report. From the model the level of the backscatter and the shape of the backscatter versus grazing angle curve depend principally on the size of surface roughness, the ratio of sediment acoustic impedance to that of water, and a volume scattering coefficient. Other model parameters may be replaced by constants. The Kirchhoff approximation describes well the surface backscatter component, for all but the very roughest surfaces. It is concluded that it should be possible to seperately estimate the surface roughness height, the volume backscatter and the sediment's acoustic impedance from acoustic returns. Sediment impedance is well correlated with other sediment properties which can then be estimated.

RELEASE LIMITATION

Approved for public release

DEPARTMENT OF DEFENCE
DEFENCE SCIENCE & TECHNOLOGY ORGANISATION
DSTO

Published by

DSTO Aeronautical and Maritime Research Laboratory
PO Box 4331
Melbourne Victoria 3001 Australia

Telephone: (03) 9626 7000
Fax: (03) 9626 7999

AR-011-565
September 2000

APPROVED FOR PUBLIC RELEASE

Modelling Acoustic Backscatter from Near-Normal Incidence Echosounders - Sensitivity Analysis of the Jackson Model

Executive Summary

Knowledge of seabed properties, such as sediment type, grain size, bulk density and sound speed, is required for predictions of mine burial and the detection ranges of sea mines. For a number of years devices have been fitted to ships' echosounders that analyse the level and shape of the acoustic returns to infer bottom types. Commercial examples are RoxAnn and QTC-View. The methods used by these systems are generally highly empirical. Careful calibrations have to be carried out to relate particular echo shapes to particular bottom types. The calibrations thus found are specific to a particular echosounder and are for a single location. For instance, a calibration carried out in Sydney Harbour, over a range of bottom types, may be of no use for surveying sediments in Torres Strait.

In an effort to reduce the empiricism involved in using echosounders for acoustic seabed classification the physics of acoustic backscatter at near-vertical grazing angles is being investigated. In this report a well established mathematical model (the Jackson model) is used to investigate the main mechanisms affecting backscatter at these angles in order to determine what sediment properties can reasonably be expected to be inferred from echosounder systems. The modelling is done for a frequency of 50 kHz, a typical frequency for ship's echosounders. For sediments composed of mud (i.e silts and clays) the returns are dominated by backscatter from inhomogeneities within the sediment body; for fine sands both surface roughness and volume inhomogeneities are important; for all coarser sediments only the surface roughness matters. The size of the surface roughness is far more important than the length scale of the surface inhomogeneities. The overall level of acoustic backscatter increases as ρv increases, where ρv is the ratio of the product of the sediment density and sound speed to the same product for water. There are thus three principal factors determining acoustic backscatter, each of which is parameterised in the Jackson model. Other model parameters can be replaced by constants. From the shape and level of the backscatter versus grazing angle curve it should be possible to estimate the three principal parameters from real data. As ρv is well correlated with other sediment properties it would be possible to determine these also.

The data obtained from an echosounder are backscatter versus time, not grazing angle. A treatment of this will be the subject of a subsequent report, and at that stage methods to extract values of ρv, roughness height and volume scattering coefficient will be developed. One important conclusion arising from a preliminary examination of the shape of backscatter versus grazing angle curves is that backscatter changes little for grazing angles between 70° and 20°. Therefore, if one only wants an indicator, or index, of backscatter levels for estimating acoustic detection ranges, the tail of the output from

a ship's echosounder, which corresponds to grazing angles near 65° or 70°, could be used, either in real-time or for route surveys.

The benefits of this work to mine countermeasures and route surveying are that it will be possible to provide improved inputs to mine burial prediction models and to probability of mine detection algorithms. This should result in increased speed and certainty in mine clearance operations. For Australian industry there exists the possibility of developing improved acoustic seabed classification systems.

Contents

1. Introduction

The conduct of mine hunting operations is very much influenced by a number of environmental factors and amongst these one of the most important is the nature of the sea floor. Acoustic backscatter from the seabed has a major influence on the detection probability of ground mines, and if a mine becomes buried or partly buried it can be extremely difficult to detect. A number of acoustic systems have been developed for classifying the seabed, prominent ones being RoxAnn (Murphy et al, 1995) and QTC-View (Collins et al, 1996). These systems are attached in parallel to the output of a standard ship's echosounder and analyse the acoustic returns from the seabed in various ways. The relationships they obtain between features of the acoustic returns and seabed properties are empirical and site specific, and they always require a certain amount of ground truthing to correlate seabed parameters with acoustic features (Hamilton et al, 1999).

A number of mathematical models have been developed in recent years in order to gain a better physical understanding of acoustic backscatter from the sea floor. Models that consider backscatter versus grazing angle include those of Stockhausen (1963), Crowther (1983), Stanton (1984), Jackson et al (1986), and Boyle and Chotiros (1995). Models which consider the behaviour of backscatter versus time, from a pulse transmission, include those of Bergem et al (1999) and Clarke et al (1988). The model of Jackson et al (1986) is one of the most widely used for backscatter versus grazing angle. It has a large body of experimental data from a range of different environments to support it. Jackson et al (1986) state that the model is valid in the frequency range 10 kHz to 100 kHz.

In this report the theory of Jackson et al (1986), herein called "the Jackson model", is used to model the nature of the acoustic returns from a near-normal incidence echosounder of the type used for acoustic seabed classification, to determine which parameters are most important for particular bottom types. (Details of this model are also in Applied Physics Laboratory, 1994). The aim here is to determine the type of information to be expected from the acoustic returns of a near-normal incidence echosounder, so as to improve the physical basis for acoustic seabed classification and to determine if the amount of empiricism currently required can be reduced.

2. Summary of the Jackson Model

The Jackson model calculates backscatter as a function of grazing angle, not backscatter as a function of time, as seen by echosounders. It models the total backscatter, from the sediment surface and below it, returning to an acoustic transponder from a narrow beam which strikes an element of the sea floor, at a grazing angle θ, as sketched in Figure 1. In contrast the signal obtained with a broad beam echosounder, of the type used with acoustic seabed classification systems, is obtained as a function of time.

Hence, at any one time, contributions are made to the return signal both from the sediment surface and from volume inhomogeneities within the sediment. Details of the geometry of the ensonified volume as it changes with time are in Clarke and Hamilton (1999). The Jackson model is used here because it helps to clarify the magnitude of different backscatter processes for different sediment types. The modelling of backscatter as a function of time, for a near-normal incidence echosounder, will be the subject of a subsequent report that uses the simplifications arising out of this one.

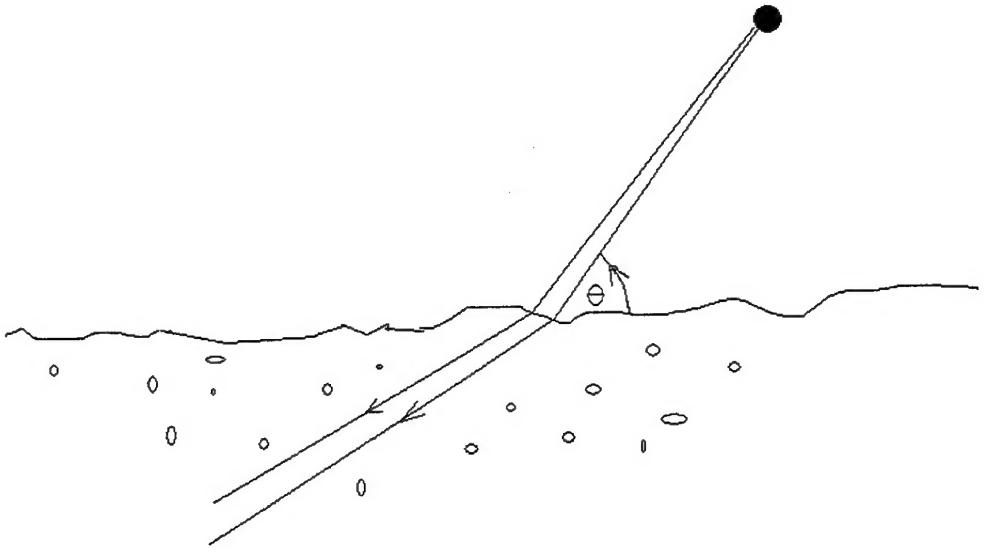

Figure 1. Sketch of geometry for backscatter versus grazing angle models.

The Jackson model splits seabed acoustic backscatter into two parts – that from the sediment-water interface and that from volume inhomogeneities within the sediment. Although Lyons et al. (1994) have extended the Jackson model to include interfaces within the sediment body, this feature will not be considered here, and the sediment body will be assumed to be homogeneous, but with some volume scattering cross section, σ_v.

2.1 Model's Input Parameters

The six parameters controlling the backscatter from the water-sediment interface are:

ρ = the ratio of sediment mass density to water mass density, also called density ratio;

ν = the ratio of sediment sound speed to water sound speed, also called sound speed ratio;

δ = the ratio of imaginary wavenumber to real wave number for the sediment, (it is related to the sound attenuation coefficient), also called loss parameter;

γ = the exponent of the power-law, bottom relief spectrum, also called spectral exponent;

β = the magnitude of the bottom relief spectrum (cm^4) at a wavenumber of 1 cm^{-1}, also called spectral strength.

(The bottom relief spectrum, $W(k_r)$, is assumed to be of the form $W(k_r) = \beta k_r^{-\gamma}$, where k_r is a spatial wave number).

The sediment volume backscatter is parameterised by the one variable:

σ_2 = the ratio of sediment volume scattering coefficient to sediment attenuation coefficient, also called the volume parameter.

A number of careful experiments have been carried out comparing the results of the model with at sea experimental data (Jackson et al, 1986; Mourad and Jackson, 1989; Applied Physics Laboratory, 1994; Jackson and Briggs, 1992; Jackson et al, 1996). Good agreement has been found between the two, using measured values of all the sediment surface parameters as input. However it is extremely difficult to estimate the volume parameter and it can only be used as an adjustable constant, to provide a best fit between model and data. What has been provided by these experiments is the range of values of the volume parameter to be expected in different sediments.

In most cases the sediment surface parameters ρ, ν, δ, γ and β are not known. Mourad and Jackson (1989) developed empirical relationships between each of these and the logarithmic grain size Mz, where

$$Mz = -\log_2 (d/d_0) = -3.32 \log_{10}(d/d_0), \quad (1)$$

where d = mean grain diameter (or grain size) in mm, and
d_0 = a reference length of 1 mm.

Mourad and Jackson's relationships for ρ, ν, δ, γ, β and σ_2 are listed in Appendix A and are similar to those of Hamilton and Bachman (1982). The values given in Appendix A for γ, β and σ_2 are only reasonable default values and are not tightly correlated with Mz. The values of sediment parameters used in subsequent calculations are listed in Table 1. The values for ρ, ν, δ, γ, β and σ_2 were obtained from the formulae of Appendix A and are representative values associated with each grain diameter. In this report the terms 'mean grain diameter' and 'grain size' will be used interchangeably.

Table 1. List of Sediment Parameters Values used in this Report.

Sediment Name	Mean Grain diameter (mm)	Density ratio ρ	Sound Speed Ratio ν	Loss parameter δ	Volume parameter σ_2	Spectral exponent γ	Spectral strength β (cm^4)
Clay	0.002	1.144875	0.9801043	0.0014725417	0.001; 0; 0.005	3.25	$5.175x10^{-4}$; $51.75x10^{-4}$
Silt	0.02	1.149182	0.9881798	0.005651104	0.001;0; 0.005	3.25	$5.175x10^{-4}$; $51.75x10^{-4}$
Fine sand	0.25	1.615902	1.139692	0.01610051	0.002; 0; 0.005	3.25	0.0035
Medium sand	0.5	2.151217	1.174087	0.01578149	0.002; 0; 0.005	3.25	0.00558833
Coarse sand	1.0	2.3139	1.2278	0.01566176	0.002; 0	3.25	0.008601511
Very coarse sand	2.0	2.492159	1.286925	0.01641595	0.002	3.25	0.01293447; 0.026
Gravel	--	2.5	1.5	0.014	0.002	3.25	0.014
Rock	--	2.5	2.5	0.01374	0.002	3.25	0.01862; 0.000518 0.20693

The sediment names in Table 1 are just used here as convenient labels. For example a sediment with a grain size of 0.02 mm could be a mixture of sand and silt, as could one with a grain size of 0.25 mm. Of course the proportions of silt and sand would differ.

2.2 Equations for Bottom Backscattering Strength

This section is a summary of the description of the relevant equations in Applied Physics Laboratory (1994). The bottom backscattering strength $S_b(\theta)$ depends on the six parameters described in section 2.1, the acoustic frequency, f, and the grazing angle, θ. $S_b(\theta)$ can be written as:

$$S_b(\theta) = 10\log_{10}[\sigma_r(\theta) + \sigma_v(\theta)] \qquad (2)$$

Where

$\sigma_r(\theta)$ = dimensionless backscattering cross section per unit solid angle per unit area due to surface roughness,

$\sigma_v(\theta)$ = dimensionless backscattering cross section per unit solid angle per unit area due to volume scattering from below the sediment surface.

2.2.1 Roughness scattering cross section, $\sigma_r(\theta)$

Three different approximations are used for the roughness scattering cross section in the Jackson model. For smooth and moderately rough surfaces (e.g. clay, silt and sand) the Kirchhoff approximation is used for grazing angles near 90°, and the composite roughness approximation (Brown, 1978 and 1980, McDaniel and Gorman, 1983) is used for all other angles. For rough bottoms (e.g. gravel and rock) an empirical expression from Jackson (1987) is used.

2.2.1.1 Kirchhoff Approximation

The Kirchhoff approximation applies to surfaces having arbitrary height and slope, but with a local radius of curvature, R_c, which satisfies:

$$R_c \geq \lambda / (\pi \sin^3\theta_g), \tag{3}$$

where θ_g is the local grazing angle, and λ is the wavelength of the incident sound.

In the Kirchhoff approximation, following Applied Physics Laboratory (1994), the backscattering cross section, σ_{kr}, is given by the following approximation to a full integral expression:

$$\sigma_{kr} = bq_c \, |R(90°)|^2 / \{8\pi [\cos^{4\alpha}(\theta) + a\, q_c^2 \sin^4(\theta)]^{((1+\alpha)/2\alpha)}\}, \tag{4}$$

where $\alpha = 0.5\gamma - 1$,

$q_c = C_h^2 \, 2^{1-2\alpha} \, k^{2(1-\alpha)}$,

$C_h^2 = 2\pi\beta\Gamma(2-\alpha)2^{-2\alpha} / \{h_0^{\gamma}\alpha(1-\alpha)\Gamma(1+\alpha)\}$,

$k = 2\pi/\lambda$,

h_0 = a reference height of 1 cm,

$a = [8\alpha^2 \Gamma(0.5+0.5/\alpha) / \{\Gamma(0.5)\,\Gamma(0.5/\alpha)\,\Gamma(1/\alpha)\}]^{2\alpha}$,

$b = a^{0.5+0.5/\alpha}\,\Gamma(1/\alpha) / 2\alpha$,

Γ = the gamma function,

and $R(90°) = (imp-1)/(imp+1)$, the complex Rayleigh reflection coefficient,

where $imp = \rho v/(1+\delta)$.

From Applied Physics Laboratory (1994), when the surface roughness power spectrum and the rms roughness height, h, are obtained over the same 1 m long track, β is related to h by:

$$\beta = 0.00207\, h^2, \text{ in cm}^4 \tag{5}$$

2.2.1.2 Composite Roughness Approximation

In the composite roughness approximation, the small-roughness perturbation approximation is used with corrections for shadowing and large-scale rms bottom slope (McDaniel and Gorman, 1983). For the small-roughness perturbation approximation the rms roughness height is much less than the acoustic wavelength and surface slope is small. The large-scale rms slope, s, is defined by:

$$s^2 = (2\pi\beta\, h_0^{-\gamma})^{1/\alpha}\, [k^2/\alpha]^{(1-\alpha)/\alpha}\, /\{2(1-\alpha)\} \tag{6}$$

The composite roughness cross section, σ_{cr}, can be written as:

$$\sigma_{cr} = S(\theta, s)\, F(\theta, \sigma_{pr}, s) \tag{7}$$

where $S(\theta, s)$ is the shadowing correction and $F(\theta, \sigma_{pr}, s)$ is a slope averaging integral, to be defined. Following Applied Physics Laboratory (1994),

$$S(\theta, s) = (1-e^{-2Q})/2Q \tag{8}$$

where $Q = \pi^{-0.5} \exp(-t^2) - t[1-\text{erf}(t)]\, /4t,$

and $t = \tan(\theta)/s.$

Now $F(\theta, \sigma_{pr}, s)$ is the small-roughness perturbation cross section averaged over bottom slope. It is approximated by:

$$F(\theta, \sigma_{pr}, s) = \pi^{-0.5} \sum_{n=-1}^{1} \{a_n\, \sigma_{pr}\, (\theta-\theta_n)\} \tag{9}$$

$a_{-1} = a_1 = 0.295410,\ \ a_0 = 1.181636,\ \theta_{-1} = \theta_1 = 1.224745\theta_s,\ \theta_0 = 0.0,\ \theta_s = (180s/\pi)$ degrees.

$\sigma_{pr}(\theta)$ is the bottom scattering cross section in the small-roughness perturbation approximation, and, following Kuo (1964), is given by:

$$\sigma_{pr}(\theta) = 4k^4 \sin^4(\theta)\ |Y(\theta)|^2\, \beta(K_\theta) \tag{10}$$

where $Y(\theta) = (\rho-1)^2 \cos^2(\theta) + \rho^2 - \kappa^2 / \{\rho\sin(\theta) + P(\theta)\}^2,$

$\kappa = (1+i\delta)/\nu,$

$P(\theta) = \sqrt{(\kappa^2 - \cos^2(\theta))},$

$K_\theta = [4k^2 \cos^2(\theta) + (k/10)^2]^{0.5}.$

2.2.1.3 *Large-Roughness Scattering Cross Section*

For gravel and rock bottoms the Kirchhoff and composite roughness approximations are no longer valid, and the Jackson model uses the following empirical equation for the large-roughness cross section, σ_{lr}:

$$\sigma_{lr}(\theta) = \sigma_1 \sin^m[\pi/\text{fact}] + 0.0260\,|R(90°)|^2 / \{s^2\,\text{fact}[1+(\theta-90)^2/(2.6\theta_s^2)]^{1.9}\} \qquad (11)$$

where fact = $1+0.81\,\theta_c^2/\theta^2$,
$m = 0.726s^{-1/3}$,
$\sigma_1 = 0.04682s^{1.25}v^{3.25}[(1-2/\rho)v^{-2}+1]^2 / \{1+3.54\theta_s/\theta_c\}$,

and the critical angle, θ_c, is given as:

$\theta_c = \cos^{-1}(1/v)$, for $v \geq 1.001$, and
$\theta_c = 2.5613°$, for $v < 1.001$.

2.2.1.4 *Interpolation between Approximations*

Interpolation between the different approximations uses the function f(x), where:

$$f(x) = 1/(1+e^x) \qquad (12)$$

First interpolation is carried out between the Kirchhoff and composite roughness approximations. Defining the interpolated cross section as the "medium roughness" cross section σ_{mr}, σ_{mr} is given by:

$$\sigma_{mr}(\theta) = f(x)\sigma_{kr}(\theta) + [1-f(x)]\sigma_{cr}(\theta) \qquad (13)$$

where:

$$x = 80[\cos(\theta) - \cos(\theta_{kdB})],$$

$$\cos(\theta_{kdB}) = [4+1/C_4]^{-0.25},$$

$$C_4 = (1000)^{1/(1+\alpha)}(aq_c^2)^{1/\alpha}.$$

The changeover from the Kirchhoff to the composite roughness approximation occurs approximately at the angle θ_{kdB}, at which the Kirchhoff cross section has fallen to approximately 15 dB below its value at 90°.

Next the interpolation is carried out between the large roughness and medium roughness approximations to give the final surface roughness cross section, σ_r, as:

$$\sigma_r = f(y)\sigma_{mr}(\theta) + [1-f(y)]\sigma_1 \qquad (14)$$

where

$$y = (\theta_s-\theta_r)/\Delta\theta,$$

$$\theta_r = 7°, \Delta\theta = 0.5.$$

2.2.2 Sediment volume scattering cross section, $\sigma_v(\theta)$

$\sigma_v(\theta)$ is given by:

$$\sigma_v(\theta) = S(\theta, s)\, F(\theta, \sigma_{pv}, s) \tag{15}$$

where $S(\theta, s)$ is given by equation (8) and $F(\theta, \sigma_{pr}, s)$ is given by equation (9), with σ_{pr} replaced by:

$$\sigma_{pv} = 5\delta\sigma_2 \,|\, 1\text{-}R^2(\theta) \,|^2 \sin^2(\theta)/[\nu \ln 10 \,|\, P(\theta) \,|^2 \mathrm{Im}\{P(\theta)\}] \tag{16}$$

where $P(\theta) = \sqrt{(\kappa^2 - \cos^2(\theta))}$.

3. Results for Backscatter versus Grazing Angle

From the previous section it can be seen that results from the Jackson model depend on six input parameters and a range of different physical mechanisms. In order to simplify interpretation of results, it seems worthwhile to examine the sensitivity of the model results to different input parameters as a function of sediment type. It is likely that not all six parameters will always be needed, and that some scattering mechanisms can be ignored in some cases.

To simplify the investigation, to some extent, the range of grazing angles to be considered will be that of an echosounder, with a beam width of 50°, pointing vertically downwards, and operating at a frequency of 50 kHz. Grazing angles then are greater than or equal to 65°. These specifications are used because that is the type of echosounder being used at DSTO, Sydney, to gather data. Also it will be assumed that the sea floor has no large scale slope, i.e. that it is flat, and that there are no large seabed inhomogeneities such as sand dunes, individual rocks, etc. within the ensonified area.

3.1 Model Sensitivity to the spectral exponent, γ

The spectrum, $W(k_r)$ of the seabed interface roughness has been assumed to have the form:

$$W(k_r) = \beta k_r^{-\gamma}.$$

From Applied Physics Laboratory (1994), γ is limited by theoretical and numerical considerations to $2.4 < \gamma < 3.9$, and from available experimental data γ lies between 3

and 3.5, with a mean of 3.23 and a standard deviation of 0.44. A default value of 3.25 is often used in calculations.

It will be seen below that for all sediments, except the coarsest, (grain sizes ≥ 2 mm) the Kirchhoff approximation, by itself, provides an acceptable approximation to surface scattering, for grazing angles ≥ 65°.

As before we write $\alpha = 0.5\gamma - 1$. Then for $3 < \gamma < 3.5$, we have $0.5 < \alpha < 0.75$. From equation (4), and the equations immediately following it, it can be seen that the Kirchhoff backscattering cross section, σ_{kr}, is a function of α, β, θ and $|R(90°)|$, where the last is the Rayleigh reflection coefficient and is a function of the product ρv. By looking at the ratio $\sigma_{kr}/|R(90°)|^2$ the dependence of backscatter on α, β and θ can be modelled, independently of other parameters.

Fixing β at 0.01, (equivalent to a rms roughness height of 20 mm, from equation (5)) the influence of α (or equivalently γ) on backscatter for grazing angles, θ, between 65° and 90° is shown in Figure 2. Over this range of grazing angles, at any one θ, the ratio $\sigma_{kr}/|R(90°)|^2$ only varies with α by ± 1 dB. Given the natural variability in acoustic backscatter this is negligible. For the rest of this report γ will be given the default value of 3.25, equivalent to $\alpha = 0.625$.

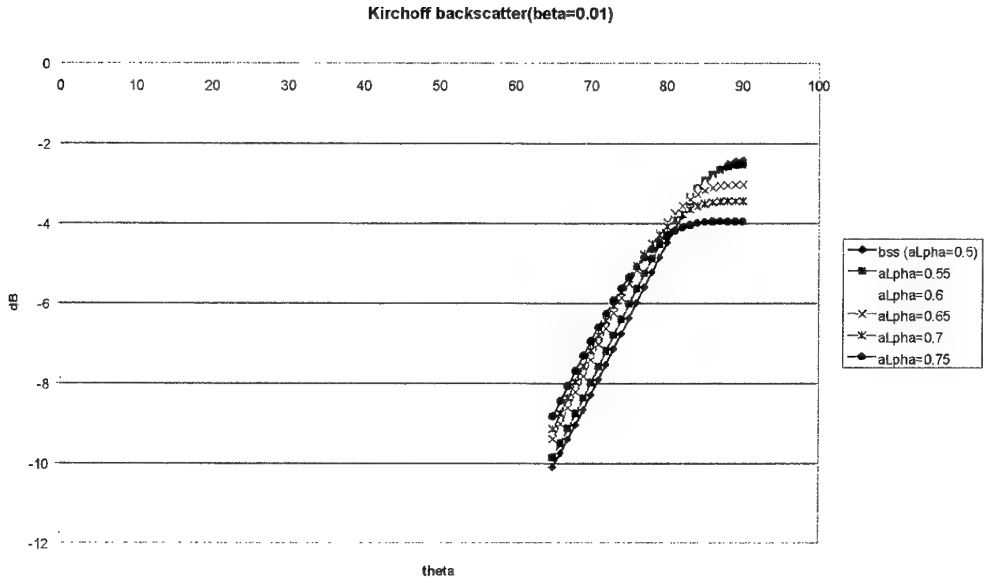

Figure 2. Ratio $\sigma_{kr}/|R(90°)|^2$ versus grazing angle for $\beta = 0.01$ and $0.5 \leq \alpha \leq 0.75$.

3.2 Model Sensitivity to the spectral strength, β

Using the same approach as in section 3.1, α was held fixed at 0.625 and the spectral strength, β, varied from 0.0005 to 0.3125, and the results are shown in Figure 3. Note that as β (i.e. the surface roughness) increases, the backscatter, represented by the ratio $\sigma_{kr}/|R(90°)|^2$, becomes less dependent on grazing angle. When β gets to 0.027951, the modelled backscatter is almost independent of grazing angle, for angles ≥ 65°. Because the backscatter curve flattens out as surface roughness increases, backscatter near 90° decreases with increasing roughness. However, for values of β > 0.013, the Kirchhoff approximation starts to break down and the large-roughness approximation should be

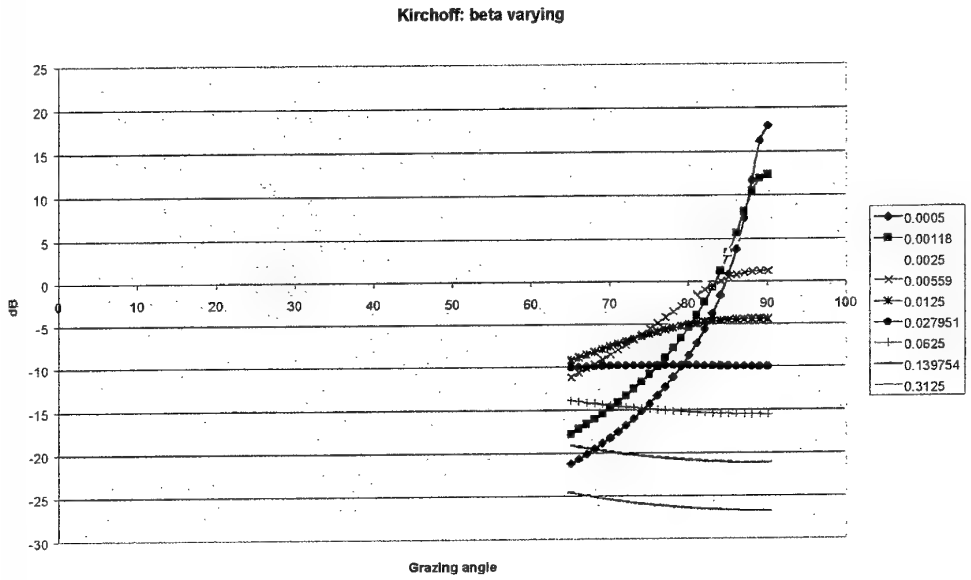

Figure 3. Ratio $\sigma_{kr}/|R(90°)|^2$ versus grazing angle for $0.0005 \leq \beta \leq 0.3125$, $\alpha = 0.625$.

used. Note the unphysical prediction of backscatter decreasing as grazing angles approach 90°, for β > 0.02795.

3.3 Model sensitivity to the Rayleigh reflection coefficient

It can be seen from equation (4) that σ_{kr} is proportional to $|R(90°)|^2$. Likewise from equation (11), when $\theta_c << \theta$, $\sigma_{lr} \propto |R(90°)|^2$. Now

$R(90°) = (imp-1)/(imp+1)$, the complex Rayleigh reflection coefficient,

where $imp = \rho v/(1+\delta)$.

Because $\delta << 1$, (See Table 1) $R(90°) \approx (\rho v - 1)/(\rho v + 1)$.

From Table 1, the normal range of values for the product ρv is 1.1 to 6.25, which means

$$0.05 \leq R(90°) \leq 0.72, \text{ and } 0.002 \leq |R(90°)|^2 \leq 0.52.$$

The ratio of 0.52 to 0.002 is 227.6, which gives a decibel range of 23.6 dB. Thus the effects of variations in ρv have an effect which is comparable to those from variations in surface roughness. Note that the spectral strength, β, (or size of the surface roughness) is roughly correlated positively with grain size as is ρv, so that the two effects will often combine.

3.4 Backscatter versus grazing angle for different sediment types.

The curves of backscatter versus grazing angle, using the recommended parameter values from Applied Physics Laboratory (1994), are displayed in Figure 4, for grazing angles from 65° to 90°. Curves for the full range of grazing angles can be found in Appendix B, for all the cases considered in this report. The recommended values are listed in Table 1. Where there are several values listed under a particular category in that table, the recommended values are the first ones. As most parameters are correlated with grain size, as in Appendix A, surface roughness generally increases with grain size. As a consequence the backscatter from finer sediments is more peaked near 90° than it is for coarser sediments, and backscatter becomes less dependant on grazing angle as grain size increases. As grain size increases the product ρv also increases, and backscatter can be seen to increase, as expected. For grazing angles between 65° and 90°, the results fall into three groups:

clay and silt, which are barely distinguishable from each other;

the four sand types and gravel, whose backscatter levels agree within ± 4 dB which is a significant range;

the two rock types.

The differences between the backscatter versus grazing angle curves for these three groups (i.e. mud, sand/gravel, rock) are sufficiently different from each other that one would expect it to be possible to distinguish between them. One factor left out of the model, at this stage, is the possible presence of small bubbles within the sediment, as discussed by Boyle and Chotiros (1995). The presence of these can lead to enhanced backscatter.

Note also that the values of backscatter at grazing angles near 65° or 70° provide a good indication of backscatter levels at lower grazing angles down to approximately 20°. This means that ordinary ships' echosounders can provide useful data to infer backscatter values applicable to quite low grazing angles.

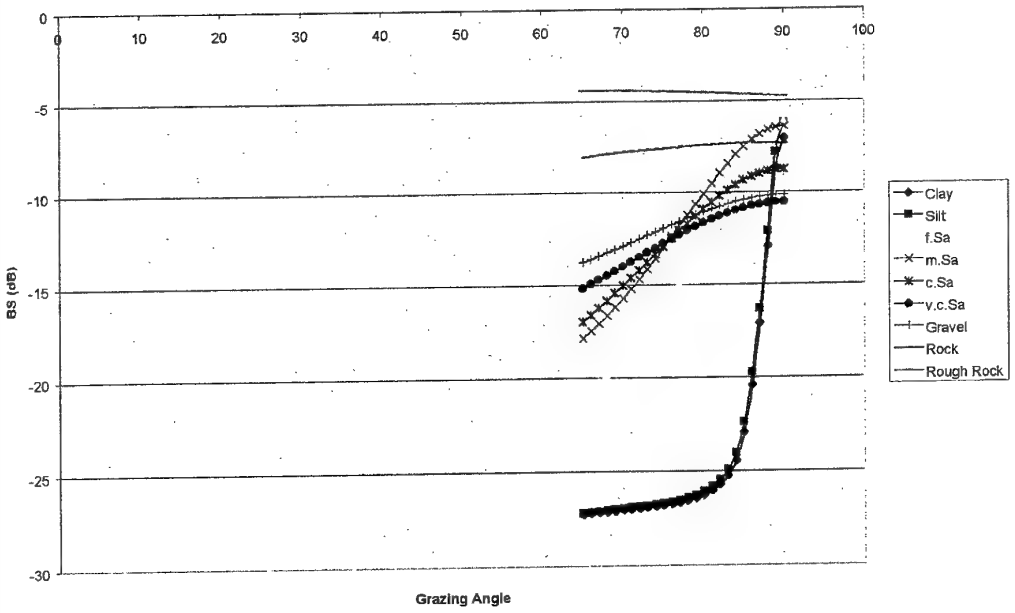

Figure 4. Backscatter versus Grazing Angle Curves for different bottom types, using recommended sediment parameters for each type.

3.4.1 Backscatter curves for Clay

Backscatter versus grazing angle curves for clay, based on different model parameters, are presented in Figure 5. In Table 2 the descriptions of the six cases considered are summarised. For Case A the whole Jackson model was used to calculate backscatter versus grazing angle. In Case B the volume contribution was unchanged but only the Kirchhoff approximation was used for the surface contribution. The difference between these curves is negligible. For Case C the whole model was used for surface scatter but there was no volume scattering. It is clear that surface scattering dominates for grazing angles greater than 80°, but volume scattering dominates for grazing angles less than 80°. For Case D the whole model was used but surface scattering was increased greatly. Case E is the same as D, except that only the Kirchhoff approximation was used for surface scattering. Cases D and E are indistinguishable from each other and they differ little from Cases A and B, except near 90°, where values are greatly reduced. In Case F volume scattering has been greatly increased but the surface scatter has been returned to its original value. There is a significant increase in backscatter compared to the other cases, except near 90°.

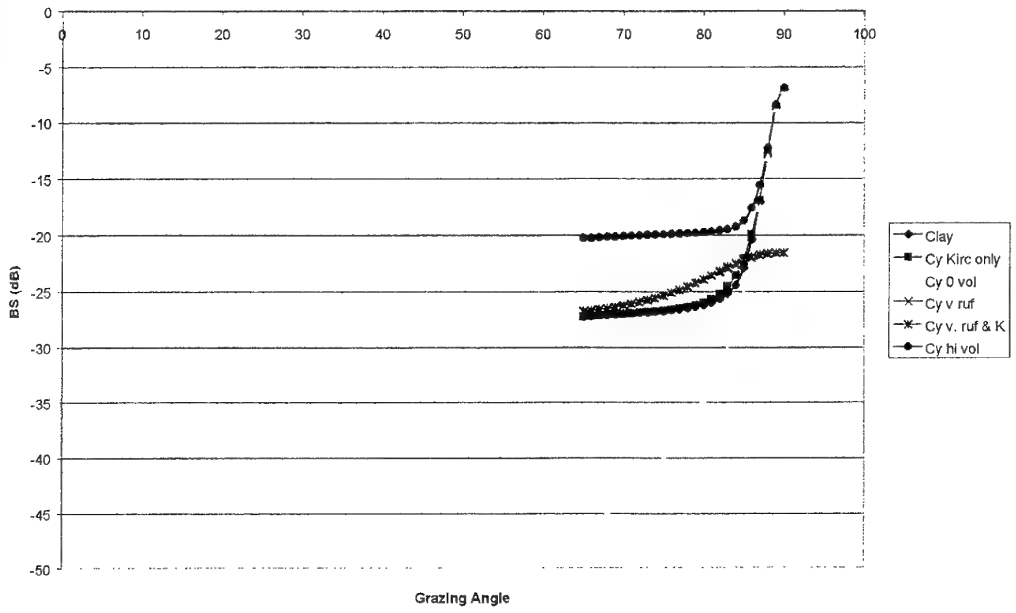

Figure 5. Backscatter versus grazing angle curves for clay.

Table 2. Descriptions of Backscatter Curves for Clay in Figure 5.

Case	Description	Label on curve	Symbol	Volume parameter	Spectral strength (cm^4)
A	Whole model	Clay	Blue diamonds	0.001	5.175×10^{-4}
B	Kirchhoff approx for surface scattering	Cy Kirc only	Pink Squares	0.001	5.175×10^{-4}
C	Whole model, no volume scattering	Cy 0 vol	Yellow triangles	0.0	5.175×10^{-4}
D	Whole model, very rough surface	Cy v. ruf	Blue crosses	0.001	51.75×10^{-4}
E	Kirchhoff approx for surface scattering, very rough surface	Cy v. ruf & K	Brown filled circles	0.001	51.75×10^{-4}
F	Whole model, high volume scattering	Cy hi vol	Purple asterisks	0.005	5.175×10^{-4}

One can conclude that for clay, the Kirchhoff approximation is perfectly adequate for modelling the surface scattering but, except near 90°, volume scattering is the dominant contributor.

3.4.2 Backscatter Curves for Silt

Backscatter versus grazing angle curves for silt are shown in Figure 6, with data on the curves in Table 3. For Case A, the whole Jackson model was used. Case B is the same, except that for surface scattering, only the Kirchhoff approximation is used. There is negligible difference between the two and the curve for Case B completely overlies that for Case A. In Case C the Kirchhoff approximation alone is used for surface scattering and volume scattering is set to zero. In Case D volume scattering is again set to zero, but the whole model is used for surface scattering. Cases C and D agree very closely but both are well below Cases A and B, except near 90°. In Case E the whole model is used with a high value of 0.005, for the volume parameter. As for clay, there is a significant increase in backscatter, except near 90°. Finally in Case F, the volume parameter is set back to 0.001, but the spectral strength of the surface roughness is increased by a factor of ten. There is little change in backscatter from the levels in Case A, except that near 90° there is a marked decrease.

The conclusions to be drawn for backscatter from silt are much the same as those for clay, i.e. that the Kirchhoff approximation provides a good model for surface scattering but, except near 90°, volume scattering dominates.

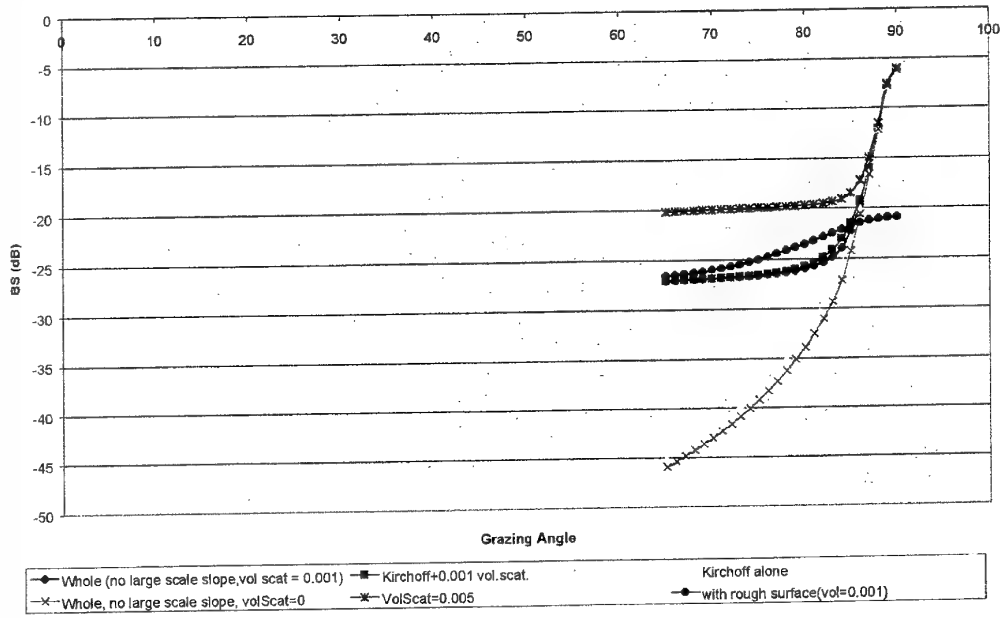

Figure 6. Backscatter versus grazing angle curves for silt.

Table 3. Descriptions of Backscatter Curves for Silt in Figure 6.

Case	Description	Label on curve	Symbol	Volume parameter	Spectral strength (cm^4)
A	Whole model	Whole (no large scale slope,vol scat=0.001	Blue diamonds	0.001	$5.175x10^{-4}$
B	Kirchhoff approx for surface	Kirchoff+0.001 vol.scat.	Pink squares	0.001	$5.175x10^{-4}$
C	Kirchhoff approx for surface, no volume scattering	Kirchoff alone	Blue crosses	0.0	$5.175x10^{-4}$
D	Whole model no volume scattering	Whole, no large scale slope, volScat=0	Purple asterisks	0.0	$5.175x10^{-4}$
E	Whole model high volume scattering	VolScat=0.005	Yellow triangles	0.005	$5.175x10^{-4}$
F	Whole model, high surface scattering	with rough surface(vol=0.001)	Brown filled circles	0.001	$51.75x10^{-4}$

3.4.3 Backscatter curves for fine sand

Model backscatter curves for a fine sand (grain size = 0.25 mm) are shown in Figure 7, with details on these curves listed in Table 4. For Case A the whole Jackson model is used, while for Case B surface scatter is obtained by only using the Kirchhoff approximation. Differences between these two curves are negligible. In Case C the whole model is used, but volume scattering is set to zero. The difference between Cases B and C is negligible near 90°, is only 2 dB at a grazing angle of 75°, but is up to 5.6 dB by 65°. That is, in the grazing angle range of 90° to 65°, volume scattering has negligible effect near 90°, but gradually becomes significant as grazing angle decreases. In Case D the volume parameter is increased to 0.005. Again this makes negligible change near 90°, but starts to be significant for grazing angles less than about 70°. The spectral strength parameter has been kept the same in all these cases. Overall, while volume scattering is important, surface scattering is the dominant factor. Again the Kirchhoff approximation provides a good description of surface scattering for grazing angles greater than 65°. Boyle and Chotiros (1995) modelled the effects of small bubbles within sand on acoustic backscatter. This can considerably enhance volume scattering, but appears not to be a major effect at grazing angles greater than 65°.

Table 4. Descriptions of Backscatter Curves for Fine Sand in Figure7.

Case	Description	Label on curve	Symbol	Volume parameter	Spectral strength (cm^4)
A	Whole model	Whole (no large scale slope)	Blue diamonds	0.002	0.0035
B	Kirchhoff approx for surface scatter	Kirchoff	Pink squares	0.002	0.0035
C	Whole model, no volume scatter	No vol scatter	Yellow triangles	0.0	0.0035
D	Whole model high volume scatter	Vol:0.005	Blue crosses	0.005	0.0035

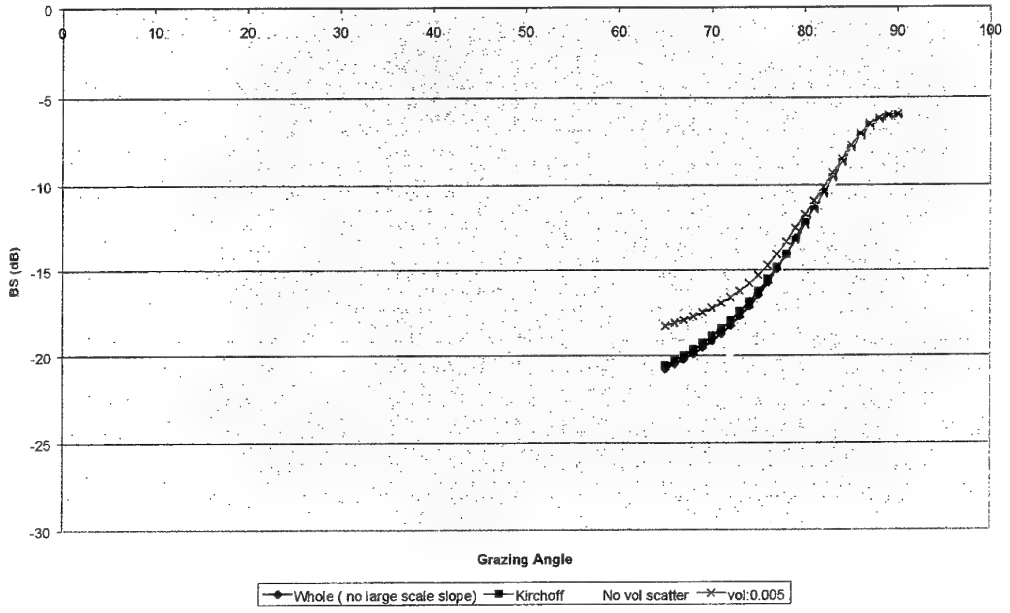

Figure 7.Backscatter versus grazing angle curves for fine sand.

3.4.4 Backscatter curves for medium sand

Backscatter versus grazing angle curves for a medium sand (grain size = 0.5 mm) are shown in Figure 8, with details on the curves tabulated in Table 5. For Case A the whole Jackson model was used. This is compared with Case B, in which volume scattering was unchanged but only the Kirchhoff approximation was used for surface scattering. Again these two cases are indistinguishable for grazing angles greater than 65°. In Case C the whole model is used but volume scattering is set to zero, while in

Case D volume scattering is put up to 0.005. The maximum difference between these curves for grazing angles ≥ 65° is only 2.3 dB. Clearly surface roughness is dominant in this case, and is well modelled using the Kirchhoff approximation.

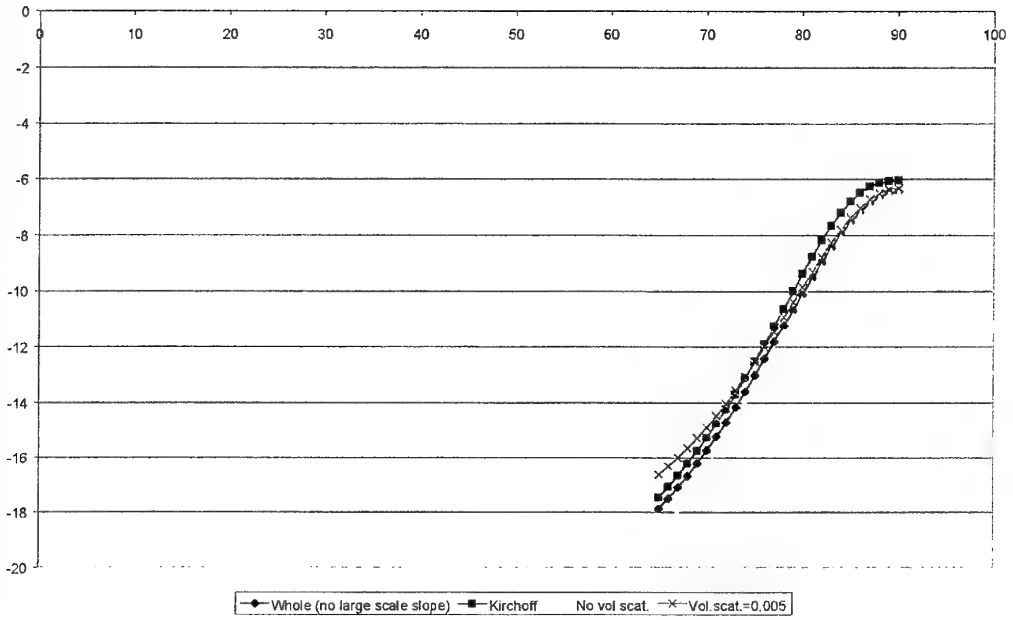

Figure 8. Backscatter versus grazing angle curves for medium sand.

Table 5. Descriptions of Backscatter Curves for Medium Sand in Figure 8.

Case	Description	Label on curve	Symbol	Volume parameter	Spectral strength (cm^4)
A	Whole model	Whole (no large scale slope)	Blue diamonds	0.002	0.0056
B	Surface scatter with only Kirchhoff approx	Kirchoff	Pink squares	0.002	0.0056
C	Whole model with zero volume scattering	No vol scat.	Yellow triangles	0.0	0.0056
D	Whole model with high volume scatter	Vol.Scat=0.005	Blue crosses	0.005	0.0056

3.4.5 Backscatter curves for coarse sand

Backscatter versus grazing angle curves for a coarse sand (grain size = 1 mm) are shown in Figure 9, and data on the curves is presented in Table 6. In Figure 9, Case A is that in which the whole Jackson model is used. In Case B volume scattering is unchanged but only the Kirchhoff approximation is used for surface scattering, while in Case C the whole model is used but volume scattering is set to zero. The difference between these curves is no more than 1.3 dB. Again surface scattering is dominant and well described by just the Kirchhoff approximation for grazing angles ≥ 65°.

Table 6. Descriptions of Backscatter Curves for Coarse Sand in Figure 9.

Case	Description	Label on curve	Symbol	Volume parameter	Spectral strength (cm^4)
A	Whole model	Whole	Blue diamonds	0.002	0.0086
B	Surface scatter with only Kirchhoff approx	Kirchoff	Pink squares	0.002	0.0086
C	Whole model with zero volume scattering	No vol scat.	Yellow triangles	0.0	0.0086

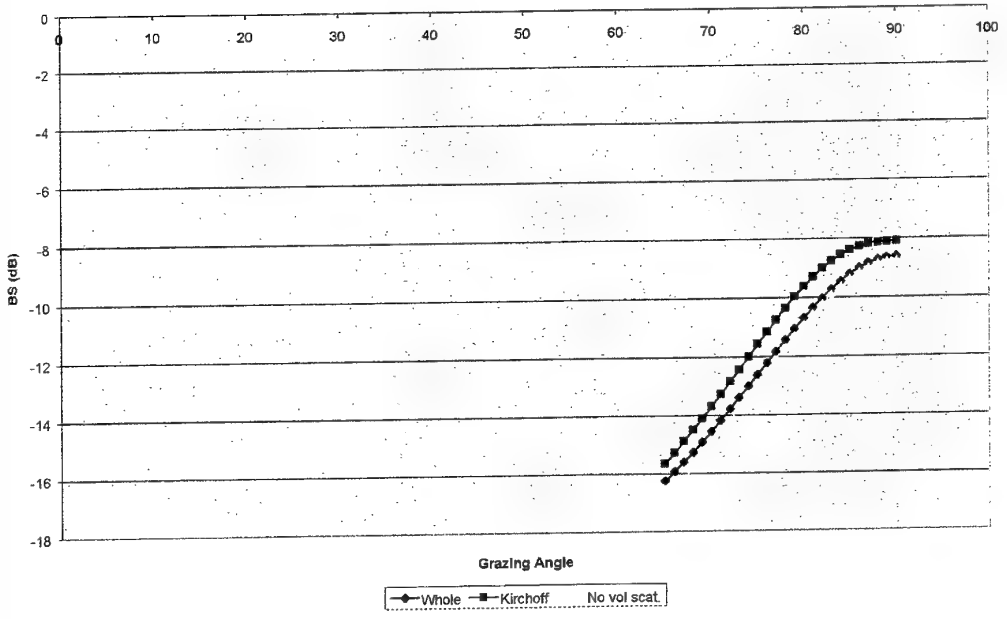

Figure 9. Backscatter versus grazing angle curves for coarse sand.

3.4.6 Backscatter curves for very coarse sand

Backscatter curves for a very coarse sand (grain size = 2 mm) are displayed in Figure 10, with data on the curves listed in Table 7. Volume scattering is the same in all six cases. Its influence will be negligible, because the surface roughness for very coarse sand is even larger than it was for coarse sand. In Case A the whole model is used, while for Case B only the Kirchhoff approximation is used for surface scattering. The two agree within 1 dB, for grazing angles ≥ 65°. For Case C both the Kirchhoff and large scale roughness approximations are used, while in Case F only the large scale roughness approximation is used. The results for Cases A, C and F are identical. For Cases D and E the surface roughness is approximately doubled. For Case D both the Kirchhoff and large roughness approximations are used, while for Case E only the Kirchhoff approximation is used. (For Case D the model carries out an interpolation between the Kirchhoff and large roughness approximations). The difference between Cases D and E is negligible for grazing angles ≥ 65°. In conclusion, at this grain size, either the Kirchhoff or large scale roughness approximation will give equally good results, although the latter is slightly more accurate. A grain size of 2 mm must be very close to the transition between the Kirchhoff and large-roughness regimes.

Table 7. Descriptions of Backscatter Curves for Very Coarse Sand in Figure10.

Case	Description	Label on curve	Symbol	Volume parameter	Spectral strength (cm^4)
A	Whole model	Whole	Blue diamonds	0.002	0.013
B	Surface scatter with only Kirchhoff approx	Kirchoff	Pink Squares	0.002	0.013
C	Kirchhoff and large roughness approx for surface scatter	Kirch&large roughness	Yellow triangles	0.002	0.013
D	Kirchhoff and large roughness approx for surface scatter – very rough case	Kirch&v.rough (hi beta)	Blue crosses	0.002	0.026
E	Surface scatter with only Kirchhoff approx –very rough case	K alone (V.rough)Hi beta	Purple asterisks	0.002	0.026
F	Large roughness approximation only, for surface scatter	Large roughness only	Brown filled circles	0.002	0.01293447

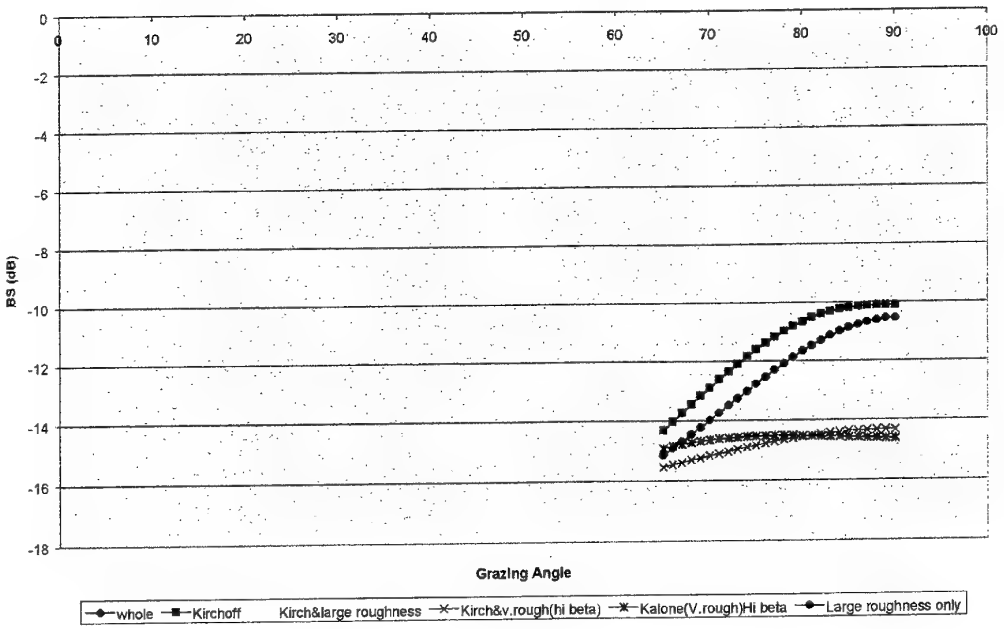

Figure 10. Backscatter versus grazing angle curves for very coarse sand.

3.4.7 Backscatter curves for gravel

Backscatter curves for gravel are shown in Figure 11, with data on them in Table 8. Both the volume and surface scatter are the same for all three curves. In Case A the whole model is used, while in Case B only the Kirchhoff approximation is used. Finally in Case C only the large roughness approximation is used. (For Case A the model carried out an interpolation between the Kirchhoff and large roughness approximations). Case C gives identical results to those in Case A, so that although all three curves are very similar, the large roughness approximation is more accurate. The same conclusion was found from the coarse sand calculations. However, for both very coarse sand and gravel, the Kirchhoff approximation still gives quite good results, for grazing angles $\geq 65°$.

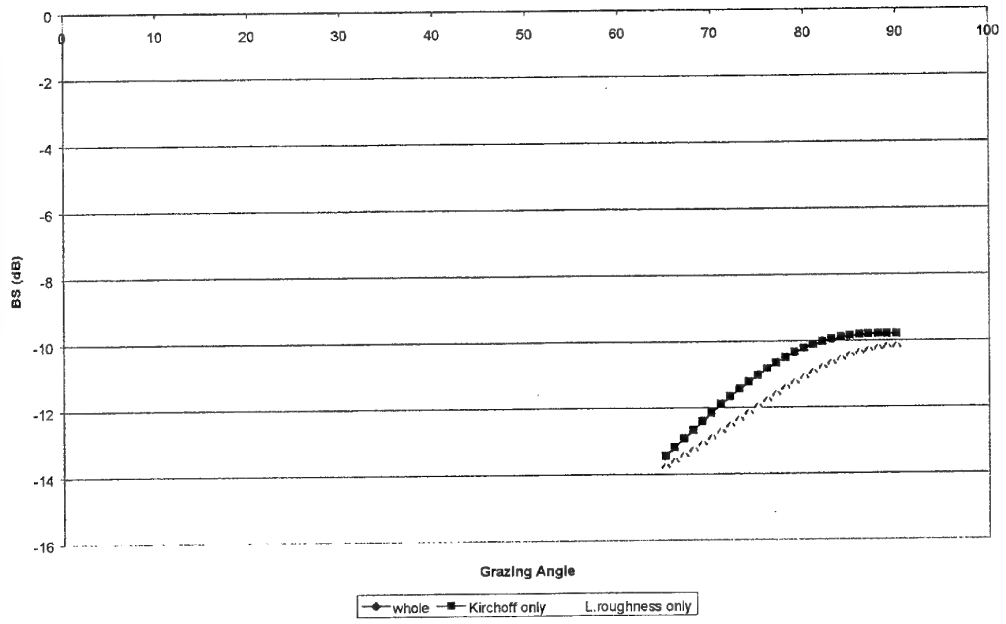

Figure 11. Backscatter versus grazing angle curves for gravel.

Table 8. Descriptions of Backscatter Curves for Gravel in Figure11.

Case	Description	Label on curve	Symbol	Volume Parameter	Spectral strength (cm^4)
A	Whole model	Whole	Blue diamond	0.002	0.014
B	Kirchhoff approximation only	Kirchoff only	Pink square	0.002	0.014
C	Large roughness approximation only	L.roughness only	Yellow triangle	0.002	0.014

3.4.8 Backscatter curves for rock surfaces

Backscatter curves for rock are presented in Figure 12, with data on the curves being tabulated in Table 9. The volume parameter, whose influence is negligible, was set at 0.002 for all these cases. For Case A the whole model was used, while in Case B only the Kirchhoff approximation was used for surface scattering. For Case C only the large roughness approximation was used. Cases A and C give identical results, while results in Case B are up to 3.9dB low, for grazing angles $\geq 65°$, indicating that the large

roughness approximation works well for a typical rock surface, while the Kirchhoff approximation does not. A rock surface with a roughness similar to silt or clay was modelled in Case D. The drastic change in the shape of the curve is quite evident. However a rock surface is very unlikely to have a surface roughness this low, except perhaps in a region which has been subject to glaciation. Such smooth rock surfaces are found off the coasts of Canada. Finally cases with large surface roughness are examined in cases E and F. In E the whole Jackson model was used, while in Case F only the large roughness approximation was used for surface scattering. As expected they agree exactly. As for gravel, the conclusion is that the large roughness approximation provides a good model for backscatter for most rock surfaces.

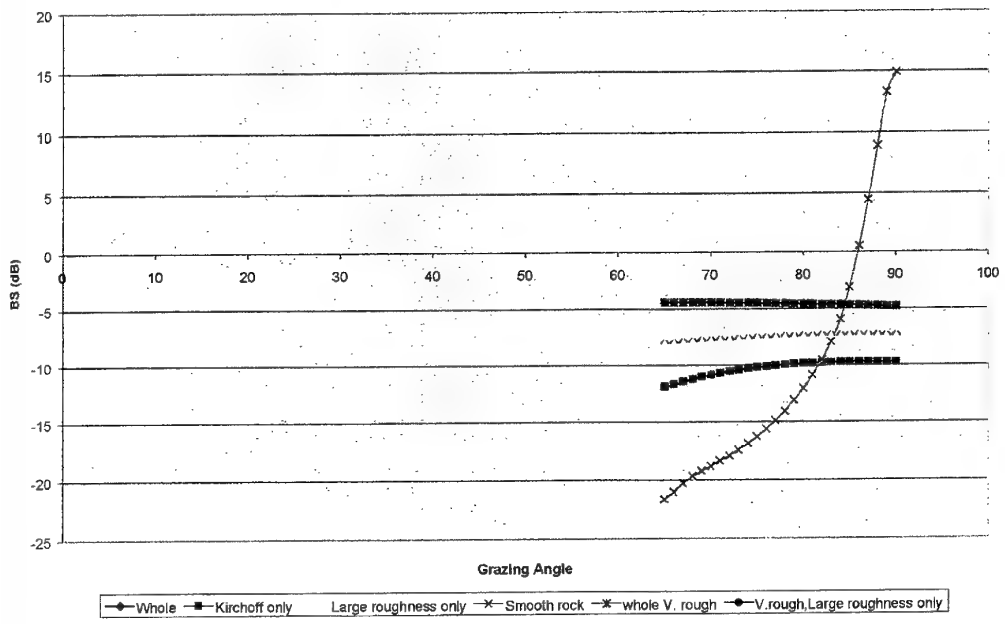

Figure 12. Backscatter versus grazing angle curves for rock.

Table 9. Descriptions of Backscatter Curves for Rock Surfaces in Figure12.

Case	Description	Label on curve	Symbol	Volume parameter	Spectral strength (cm^4)
A	Whole model	Whole	Blue diamonds	0.002	0.0186
B	Kirchhoff approximation only	Kirchoff only	Pink Squares	0.002	0.0186
C	Large roughness approximation only	Large roughness only	Yellow triangles	0.002	0.0186
D	Whole model, smooth surface	Smooth rock	Blue crosses	0.002	0.000518
E	Whole model, very rough surface	Whole V. rough	Purple asterisks	0.002	0.207
F	Very rough surface, large roughness approximation only	V.rough,Large roughness only	Brown filled circles	0.002	0.207

4. Conclusions

In section 3.1 it was shown that the spectral exponent, γ, has very little influence. In section 3.2 it was seen that the spectral strength, β, a measure of surface roughness height, had a major influence and so did the Rayleigh reflection coefficient, R(90°), over the range of experimentally found values. The roles of the different physical mechanisms in the Jackson model are summarised in Table 10, for grain sizes between 65° and 90°. For grain sizes less than or equal to 1 mm the Kirchhoff approximation by itself provides a good model for surface scattering, and even for very coarse sands and gravels it provides an acceptable model. However the large roughness approximation is probably better for the last two sediment types and it has to be used for the rougher rock surfaces.

Table 10. Summary of modelling results for different sediments. K signifies that the Kirchhoff approximation provides a good model for surface scattering; "Large roughness" implies that the large roughness approximation provides a good model for surface scattering; σ_2 implies that volume scattering must be included.

Sediment type	Grain size (mm)	Mechanisms required	Grazing angle range for Kirchhoff alone (°)
Clay	0.002 mm	K + σ_2 (dominant)	85 - 90
Silt	0.02	" "	85 - 90
Fine Sand	0.25	K (dominant) + σ_2	70 - 90
Medium Sand	0.5	K only	40 - 90
Coarse Sand	1.0	" "	"
Very Coarse Sand	2.0	Large roughness, but K good.	50 - 90
Gravel		Large roughness, but K good.	50 - 90
Rock		Large roughness	

Volume backscatter needs to be included for grain sizes ≤ 0.25 mm, and is the dominant backscatter mechanism for silt and clay. For grazing angles near 90°, only surface scattering is important even for fine sediments. These conclusions apply for a frequency of 50 kHz and for grazing angles greater than 65°. At higher frequencies volume scattering would be even less important.

From the above it can be seen that the dominant mechanisms affecting backscatter from near-normal incidence echosounders are:

(a) the size of surface roughness, specified by β, surface backscatter being adequately predicted by the Kirchhoff approximation in most cases;
(b) the product ρv (= ratio of sediment to water acoustic impedance);
(c) volume backscatter, specified by σ_2.

The level and shape of the backscatter versus grazing angle curve is thus specified by only 3 parameters, except for cases with very large roughnesses. It should be possible to estimate these from real data on backscatter versus grazing angle. However this exercise will be considered as part of a subsequent study into backscatter versus time, received from a pulsed echosounder. As a general rule, as ρv increases the overall level of backscatter increases, while as surface roughness increases the backscatter versus grazing angle flattens out, and there is less of a peak near 90°. For muds, volume scattering becomes important and separating the effects of volume and surface scattering appears to be less simple. However this may become feasible when looking at backscatter versus time because, over muds, volume returns will continue after surface backscatter returns have ceased. Also near 90° the backscatter is dominated by surface scattering. The consideration of practical algorithms to extract bottom types

from echosounder returns, and the modelling of backscatter versus time will be the subject of future reports. Some preliminary work is reported in Clarke and Hamilton (1999).

Note also, from the curves in Appendix B, that the values of backscatter at grazing angles near 65° or 70° provide a good indication of backscatter levels at lower grazing angles down to approximately 20°. Therefore, if one only wants an indicator, or index, of backscatter levels for estimating acoustic detection ranges, the tail of the output from a ship's echosounder, which corresponds to grazing angles near 65° or 70°, could be used, either in real-time or for route surveys.

5. Acknowledgments

The computer code used for most of the calculations in this report was originally obtained as a Fortran program from the Applied Physics Laboratory, University of Washington, under the TTCP program. It was then modified by Ms Jane Cleary and further modified by Mr Les Hamilton, both of the Maritime Operations Division, DSTO. Les Hamilton is especially thanked for his assistance with the computing.

6. References

Applied Physics Laboratory (1994) *APL – UW High Frequency Ocean Environmental Acoustic Models Handbook* Technical Report APL-UW TR-9407, October 1994, Applied Physics Laboratory, University of Washington, Seattle.

Bergem, O., Pouliquen, E., Canepa, G. and Pace, N. G. (1999) Time-evolution modelling of seafloor scatter. I. Concept. *J. Acoust. Soc. Am.* **105**, 3136 – 3141.

Boyle, F.A. and Chotiros, N.P. (1995) A model for high-frequency backscatter from gas bubbles in sandy sediments at shallow grazing angles. *J. Acoust. Soc. Am.* **98**, 531 – 541.

Brown, G. S. (1978) Backscattering from a Gaussian-distributed, perfectly conducting rough surface, *IEEE Trans. Antennas Propagat.* **26**, 472-482.

Brown, G. S. (1980) Correction to backscattering from a Gaussian-distributed, perfectly conducting rough surface, *IEEE Trans. Antennas Propagat.* **28**, 943-946.

Clarke P.A. and Hamilton L.J. (1999). *Analysis of Echo Sounder Returns for Acoustic Bottom Classification.* DSTO General Document DSTO-GD-0215. 42pp.

Clarke, T. L., Proni, J.R., Seem, D.A. and Tsai, J.J. (1988) *Joint CGS-AOML (Charting and Geodetic Service – Atlantic Oceanographic and Meteorological Laboratory) Acoustical Bottom Echo-Formation Research I: Literature Search and Initial Modelling Results.* NOAA Technical Memorandum ERL AOML-66

Collins, W., Gregory, R. and Anderson, J. (1996) A Digital Approach to Seabed Classification, *Sea Technology*, **37**, (8), 83-87.

Crowther, P.A. (1983) *Some statistics of the sea-bed and scattering therefrom*, in Pace, N.G. (editor) *Acoustics and the Sea-Bed*, Bath University Press, Bath, U.K.

Hamilton, E. L. and Bachman, R. T. (1972) Sound velocity and Related Properties of Marine Sediments, *J. Acoust. Soc. Am.* **72**, 1891 - 1904.

Hamilton, L.J., Mulhearn, P.J. and Poeckert, R. (1999) Comparison of RoxAnn and QTC-View acoustic bottom classification system performance for the Cairns area, Great Barrier Reef, Australia, *Continental Shelf Res.* **19**, 1577-1597.

Jackson, D. R. (1987) *Third Report on TTCP Bottom Scattering Measurements: Model Development*, APL-UW Report APL–UW 8708, September 1987, Applied Physics Laboratory, University of Washington, Seattle

Jackson, D. R. and Briggs, K. B. (1992) High-frequency bottom backscattering: Roughness versus sediment volume scattering. *J. Acoust. Soc. Am.* **92**, 962 - 977.

Jackson, D. R., Briggs, K. B., Williams, K. L. and Richardson, M. D. (1996) Tests of Models for High-Frequency Backscatter. *IEEE J. Oceanic Engineering*, **21**, (4), 458 – 470.

Jackson, D.R., Winebrenner, D.P. and Ishimaru, A. (1986) Application of the composite roughness model to high-frequency bottom backscatter. *J. Acoust. Soc. Am.* **79**, 1410 - 1422.

Kuo, E. Y. (1964) Wave scattering and transmission at irregular surfaces, *J. Acoust. Soc. Am.* **36**, 2135-2142

Lyons, A.P. and Anderson, A.L. (1994) Acoustic scattering from the seafloor: Modelling and data comparison, *J. Acoust. Soc. Am.* **95**, 2441-2451.

McDaniel, S. T. and Gorman, A. D. (1983) Acoustic and radar sea surface backscatter, *J. Geophys. Res.*, **87**, 4127-4136.

Mourad, P. D. and Jackson, D. R. (1989) High Frequency Sonar Equation Model for Bottom Backscatter and Forward Loss, in *Proceedings of OCEANS '89*, IEEE, New York, 1168-1175.

Murphy, L., Leary, T. and Williamson, A. (1995) Standardizing Seabed Classification Techniques, *Sea Technology*, **36**, (7), 15-19.

Stanton, T.K. (1984) Sonar estimates of seafloor microroughness. *J. Acoust. Soc. Am.* **75**, 809 - 818.

Stockhausen, J.H. (1963) *Scattering from the Volume of an Inhomogeneous Half-space,* Rep. No. 63/9, Naval Research Establishment, Canada.

Appendix A: Sediment Parameters versus Grain Size

For density ratio:
$\rho = 0.007797*(Mz)^2 - 0.17057*Mz + 2.3139$, for $-1.0 \leq Mz < 1.0$

$\rho = -0.0165406*(Mz)^3 + 0.2290201*(Mz)^2 - 1.1069031*Mz + 3.0455$, for $1.0 \leq Mz < 5.3$

$\rho = -0.0012973 * Mz + 1.1565$, for $5.3 \leq Mz \leq 9.0$

For sound speed ratio:
$v = 0.002709*(Mz)^2 - 0.056452*Mz + 1.2278$, for $-1.0 \leq Mz < 1.0$

$v = -0.0014881*(Mz)^3 + 0.0213937*(Mz)^2 - 0.1382798*Mz + 1.3425$, for $1.0 \leq Mz < 5.3$

$v = -0.0024324*Mz + 1.0019$, for $5.3 \leq Mz \leq 9.0$

For Loss parameter, δ:
First calculate Alpha2 (whose units are decibels/m)
aLpha2 = freq * 0.4556, for $-1.0 \leq Mz < 0.0$
aLpha2 = freq * (0.4556 + 0.0245*Mz), for $0.0 \leq Mz < 2.6$
aLpha2 = freq * (0.1978 + 0.1245*Mz), for $2.6 \leq Mz < 4.5$
aLpha2 = freq * (8.0399 - 2.5228*Mz + 0.20098*$(Mz)^2$), for $4.5 \leq Mz < 6.0$
aLpha2 = freq * (0.9431 - 0.2041*Mz + 0.0117*$(Mz)^2$), for $6.0 \leq Mz < 9.5$
aLpha2 = freq * 0.0601, for $9.5 \leq Mz$.
Then:
$\delta = (aLpha2*v*3.518*freq/(40.0*\pi)$
Here freq = the operating frequency of the sonar in kHz.

For volume parameter:
$\sigma_2 = 0.002$, for $-1.0 \leq Mz < 5.5$,
$\sigma_2 = 0.001$, for $5.5 \leq Mz \leq 9.0$.

For spectral exponent:
$\gamma = 3.25$.

For spectral strength:
$h = (2.03846-0.26923*Mz)/(1.0+0.076923*Mz)$, for $-1.0 \leq Mz < 5.0$
$h = 0.5$, for $5.0 \leq Mz \leq 9.0$,
where h = the rms roughness relief, in cm, of a 1 m track, across the sediment surface.
Then:
$\beta = 0.00207*h*h* h_0*h_0$,

where h_0 = a reference height of 1 cm, and β has units of cm^4.

Appendix B: Backscatter versus Grazing Angle Curves, for 0° to 90°.

Curves for backscatter versus grazing angle, for grazing angles from 0° to 90°, are shown in this appendix for all the cases covered in this report. This is merely done for completeness. Details on curves B2 to B9 can be found in Tables 2 to 9, respectively. There is a discontinuity at 40° in some curves because, in the model, the Kirchhoff approximation is only used for angles between 40° and 90°.

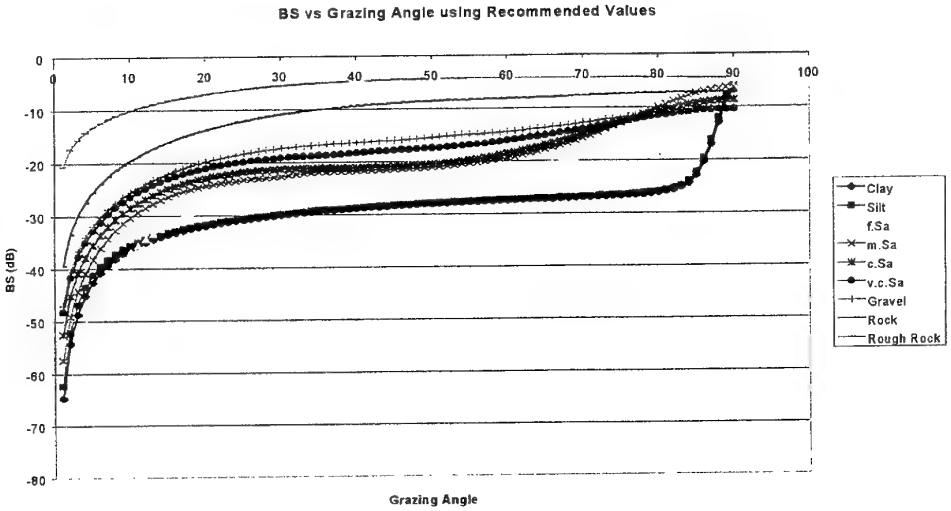

Figure B1. Backscatter versus Grazing Angle curves for different bottom types, using recommended sediment parameters for each type.

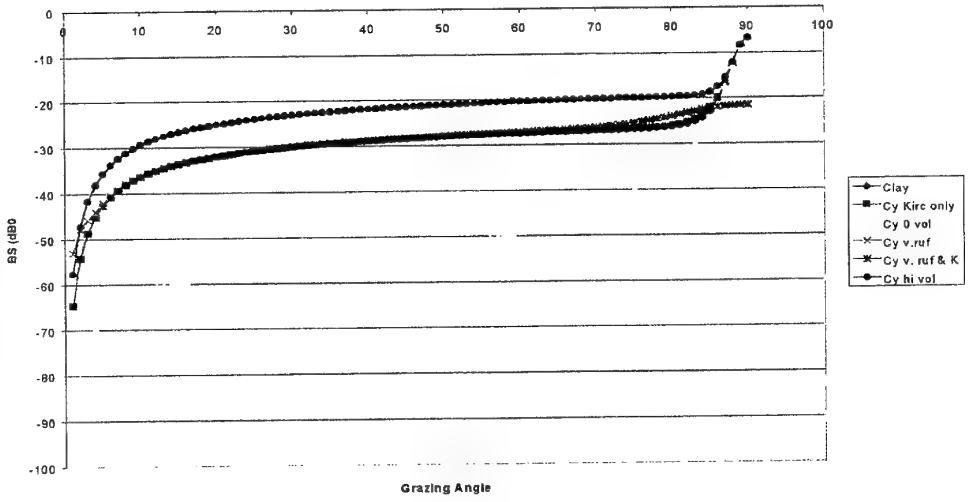

Figure B2. Backscatter versus grazing angle curves for clay.

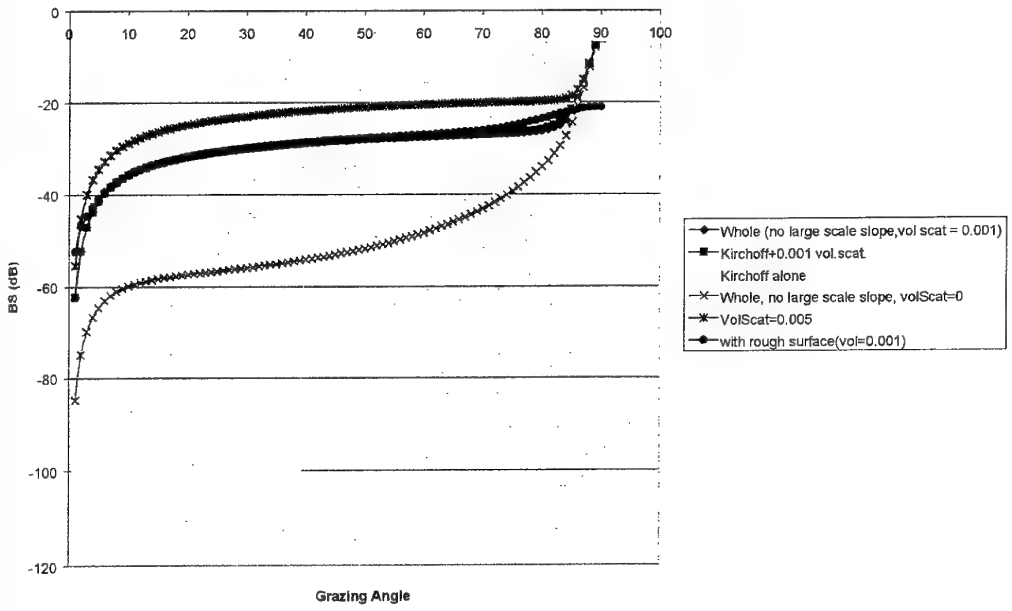

Figure B3. Backscatter versus grazing angle curves for silt.

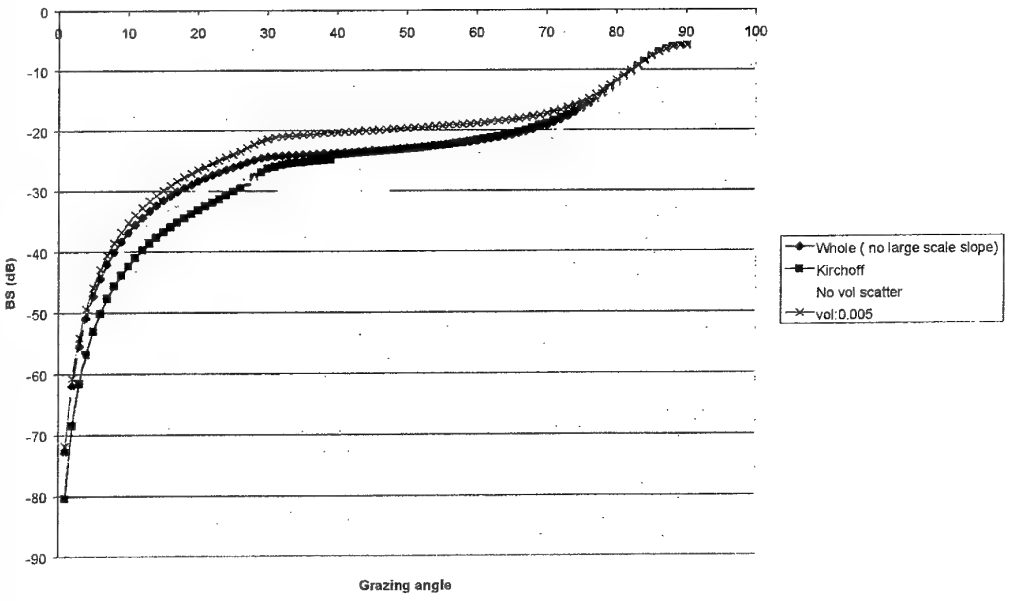

Figure B4. Backscatter versus grazing angle curves for fine sand

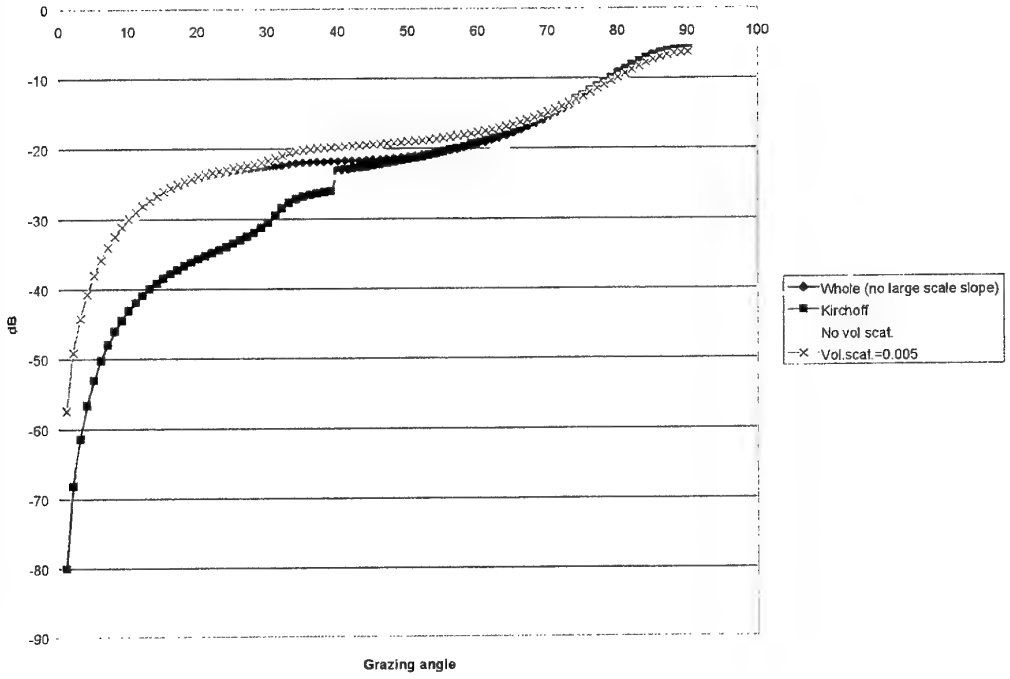

Figure B5. Backscatter versus grazing angle curves for medium sand.

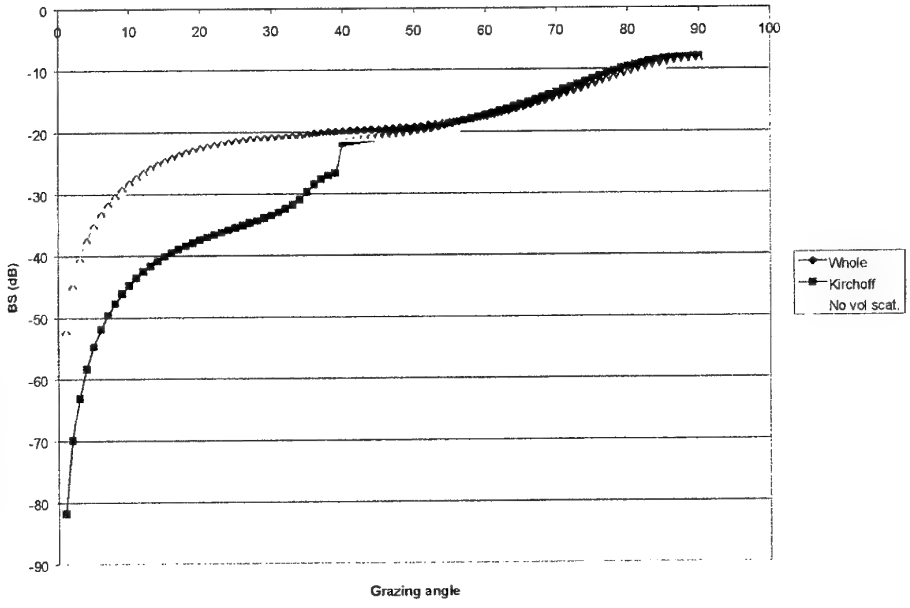

Figure B6. Backscatter versus grazing angle curves for coarse sand.

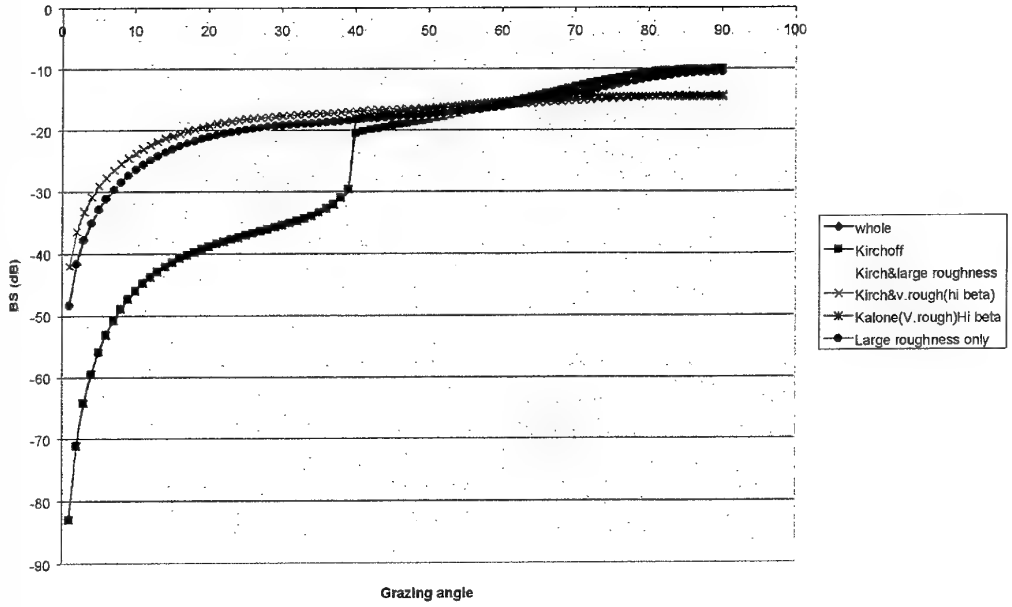

Figure B7. Backscatter versus grazing angle curves for very coarse sand.

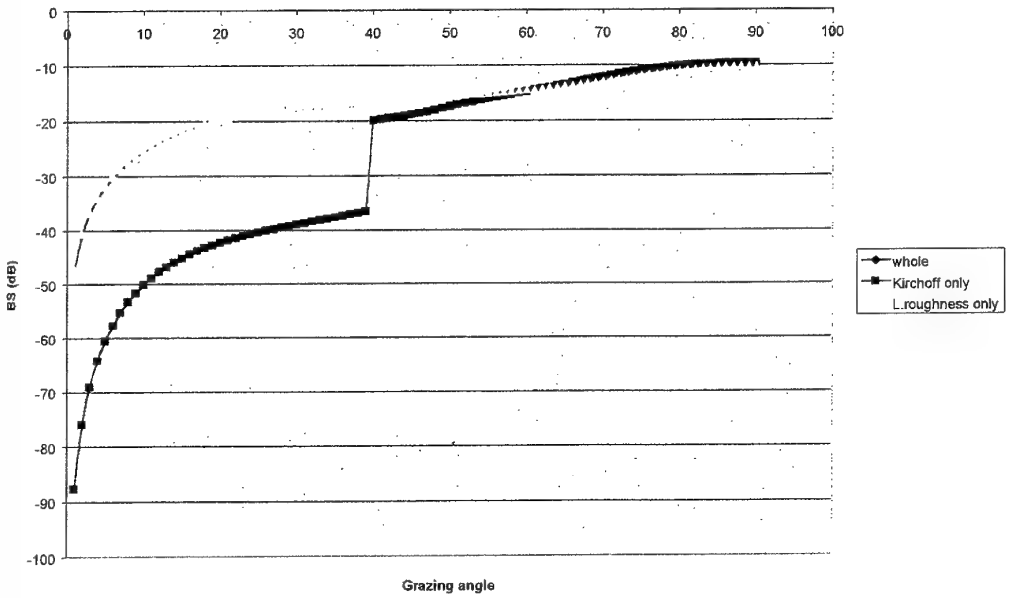

Figure B8. Backscatter versus grazing angle curves for gravel.

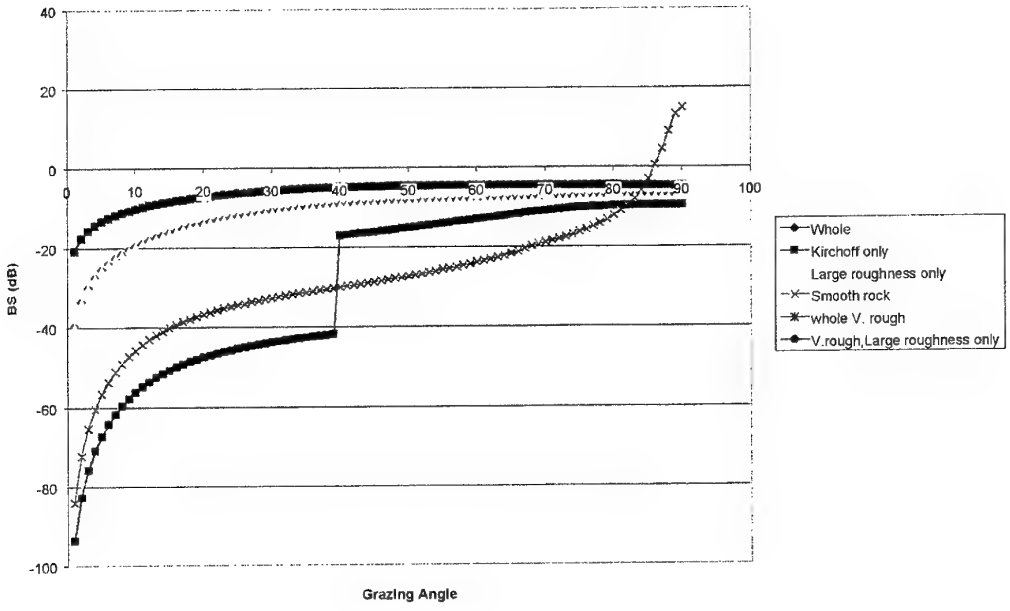

Figure B9. Backscatter versus grazing angle curves for rock.

DISTRIBUTION LIST

Modelling Acoustic Backscatter from Near-Normal Incidence Echosounders – Jackson Model

P. J. Mulhearn

AUSTRALIA

DEFENCE ORGANISATION

Task Sponsor MWCSS Project Director, DTCSS Fyshwick, Department of Defence, Canberra, ACT, 2600

S&T Program

Chief Defence Scientist
FAS Science Policy
AS Science Corporate Management
} shared copy

Director General Science Policy Development
Counsellor Defence Science, London (Doc Data Sheet)
Counsellor Defence Science, Washington (Doc Data Sheet)
Scientific Adviser to MRDC Thailand (Doc Data Sheet)
Scientific Adviser Policy and Command
Navy Scientific Adviser
Scientific Adviser - Army (Doc Data Sheet and distribution list only)
Air Force Scientific Adviser
Director Trials

Aeronautical and Maritime Research Laboratory

Director
Chief of Maritime Operations Division
Research Leader: Dr A. Theobald
Head: Dr D. H. Cato
Task Manager: Dr P. J. Mulhearn
Dr B. Ferguson
Dr S. Anstee
Dr P. Chapple
Mr L. J. Hamilton
Dr R. Neill

DSTO Library and Archives

Library Fishermans Bend (Doc Data Sheet)
Library Maribyrnong (Doc Data Sheet)
Library Salisbury (2 copies)
Australian Archives
Library, MOD, Pyrmont (2 copies)
Library, MOD, HMAS Stirling
US Defense Technical Information Center, 2 copies
UK Defence Research Information Centre, 2 copies
Canada Defence Scientific Information Service, 1 copy
NZ Defence Information Centre, 1 copy

National Library of Australia, 1 copy

Capability Systems Staff

Director General Maritime Development
Director General C3I Development (Doc Data Sheet only)
Director General Aerospace Development (Doc Data Sheet only

Navy

SO (Science), Director of Naval Warfare, Maritime Headquarters Annex, Garden Island, NSW 2000. (Doc Data Sheet only) COMAUSMINDIVFOR, HMAS Waterhen, Waverton, NSW, 2060
Director, Oceanography & Meteorology, Maritime Headquarters, Potts Point, NSW, 2011
Minehunter Coastal Project Director, Department of Defence, Campbell Park, (CP2-3-16), CANBERRA, ACT, 2600
DDMWD, A - 3-02, Russel Offices, Canberra ACT 2600
OIC, Mine Warfare School, HMAS Waterhen, WAVERTON NSW 2060
OIC, Mine Warfare Diving School, HMAS Penguin, Balmoral Naval Post Office, BALMORAL NSW 2091
Australian Project Officer, MWDDEA 5807/5819, Maritime Headquarters Annex, Garden Island, NSW 2000
Officer in Charge, RAN Clearance Diving 1, HMAS Waterhen, Waverton, NSW 2060

Army

ABCA Standardisation Officer, Puckapunyal, (4 copies)
SO (Science), DJFHQ(L), MILPO Enoggera, Queensland 4051 (Doc Data Sheet only)

Intelligence Program

DGSTA Defence Intelligence Organisation
Manager, Information Centre, Defence Intelligence Organisation

Corporate Support Program

OIC TRS, Defence Regional Library, Canberra

UNIVERSITIES AND COLLEGES

Australian Defence Force Academy
Library
Head of Aerospace and Mechanical Engineering
Hargrave Library, Monash University (Doc Data Sheet only)
Librarian, Flinders University
Dr C. Jenkins, Dept of Geology & Geophysics, University of Sydney

OTHER ORGANISATIONS

NASA (Canberra)
AusInfo

OUTSIDE AUSTRALIA

ABSTRACTING AND INFORMATION ORGANISATIONS

Library, Chemical Abstracts Reference Service
Engineering Societies Library, US

Materials Information, Cambridge Scientific Abstracts, US
Documents Librarian, The Center for Research Libraries, US

INFORMATION EXCHANGE AGREEMENT PARTNERS

Acquisitions Unit, Science Reference and Information Service, UK
Library - Exchange Desk, National Institute of Standards and Technology, US

Dr M. D. Richardson, Stennis Space Center, MS 39529-5004, USA
Mr Dan Lott, NRL, Stennis Space Center, MS 39529-5004, USA
Dr D. R. Jackson, APL, University of Washington, Seattle, WA, USA
Dr N. Chotiros, ARL, University of Texas, Austin, TX, USA
Dr R. Kuwahara, Defence Research Establisment Atlantic, Dartmouth, NS, Canada
Dr R. Holtkamp, DOTSE, Auckland Naval Base, Devenport, Auckland, NZ
Dr G. Heald, DERA, Bincleaves, Newton Road, Weymouth, UK
CMDR C. Butler, Office of Naval Research International Field Office – Europe,
223 Old Marylebone Rd, London NW1 5TH, UK

SPARES (5 copies)

Total number of copies: **74**

DEFENCE SCIENCE AND TECHNOLOGY ORGANISATION
DOCUMENT CONTROL DATA

1. PRIVACY MARKING/CAVEAT (OF DOCUMENT)

2. TITLE

Modelling Acoustic Backscatter from Near-Normal Incidence Echosounders - Sensitivity Analysis of the Jackson Model

3. SECURITY CLASSIFICATION (FOR UNCLASSIFIED REPORTS THAT ARE LIMITED RELEASE USE (L) NEXT TO DOCUMENT CLASSIFICATION)

Document	U
Title	U
Abstract	U

4. AUTHOR(S)

P. J. Mulhearn

5. CORPORATE AUTHOR

Aeronautical and Maritime Research Laboratory
PO Box 4331
Melbourne Vic 3001 Australia

6a. DSTO NUMBER	6b. AR NUMBER	6c. TYPE OF REPORT	7. DOCUMENT DATE
DSTO-TN-0304	AR-011-565	Technical Note	September 2000

8. FILE NUMBER	9. TASK NUMBER	10. TASK SPONSOR	11. NO. OF PAGES	12. NO. OF REFERENCES
490-6-581	NAV 98/026	MWCSSPD	39	22

13.URL on the World Wide Web:
http://www.dsto.defence.gov.au/corporate/reports/DSTO-TN-0304.pdf

14. RELEASE AUTHORITY

Chief, Maritime Operations Division

15. SECONDARY RELEASE STATEMENT OF THIS DOCUMENT

Approved for public release

OVERSEAS ENQUIRIES OUTSIDE STATED LIMITATIONS SHOULD BE REFERRED THROUGH DOCUMENT EXCHANGE, PO BOX 1500, SALISBURY, SA 5108

16. DELIBERATE ANNOUNCEMENT
No Limitations

17. CASUAL ANNOUNCEMENT Yes

18. DEFTEST DESCRIPTORS

acoustic scattering, underwater acoustics, backscattering, ocean bottom, echo sounding, underwater sound reverberation, high frequency

19. ABSTRACT

For a number of years systems, such as RoxAnn and QTC-View, have been attached to ships' echosounders in order to estimate sediment bottom types from the acoustic returns. In this report the physics of acoustic backscatter is examined, at near-normal incidence grazing angles, to determine if these systems can be made less empirical. The Jackson model is used to examine backscatter versus grazing angle, for angles between 65 and 90 degrees, at a frequency of 50 kHz. This is a typical frequency for a standard ship's echosounder. Backscatter predicted by the Jackson model depends on six input parameters and a range of different physical mechanisms. In order to simplify interpretation of results, it seems worthwhile to examine the sensitivity of the model results to different input parameters as a function of sediment type. It is likely that not all six parameters will always be needed, and that some scattering mechanisms can be ignored in some cases. Backscatter versus time for a pulsed system will be examined in a subsequent report. From the model the level of the backscatter and the shape of the backscatter versus grazing angle curve depend principally on the size of surface roughness, the ratio of sediment acoustic impedance to that of water, and a volume scattering coefficient. Other model parameters may be replaced by constants. The Kirchhoff approximation describes well the surface backscatter component, for all but the very roughest surfaces. It is concluded that it should be possible to seperately estimate the surface roughness height, the volume backscatter and the sediment's acoustic impedance from acoustic returns. Sediment impedance is well correlated with other sediment properties which can then be estimated.